Probing the ρ spectral function in hot and dense nuclear matter by dileptons *

W. Cassing[1], E. L. Bratkovskaya[1], R. Rapp[2] and J. Wambach[3]

[1]Institut für Theoretische Physik, Universität Giessen
D-35392 Giessen, Germany
[2] Department of Physics and Astronomy, State University of New York,
Stony Brook, NY 11794-3800, U.S.A.
[3] Insitut für Kernphysik, TU Darmstadt, Schloßgartenstr. 9,
D-64289 Darmstadt, Germany

Abstract

We present a dynamical study of e^+e^- and $\mu^+\mu^-$ production in proton-nucleus and nucleus-nucleus collisions at CERN-SPS energies on the basis of the covariant transport approach HSD employing a momentum-dependent ρ-meson spectral function that includes the pion modifications in the nuclear medium as well as the polarization of the ρ-meson due to resonant $\rho-N$ scattering. We find that the experimental data from the CERES and HELIOS-3 Collaborations can be described equally well as within the dropping ρ-mass scenario. Whereas corresponding dilepton q_T-spectra are found to be very similar, the inclusive dilepton yield in the invariant mass range $0.85 \leq M \leq 1.0$ GeV should allow to disentangle the two scenarios experimentally.

PACS: 25.75+r 14.60.-z 14.60.Cd
Keywords: relativistic heavy-ion collisions, leptons

*Work supported by BMBF and GSI Darmstadt.

1 Introduction

The mechanism of chiral symmetry restoration at high baryon density is of fundamental importance for the understanding of QCD [1, 2], but a clear experimental evidence has not been achieved, so far. Enhanced antikaon yields at SIS energies - as compared to transport studies using bare kaon masses [3, 4] - point in this direction, but the present knowledge on the elementary production cross sections close to threshold – especially for the ΔN production channel – does not yet allow for final conclusions. On the other hand, dileptons are particularly well suited for an investigation of the early phases of high-energy heavy-ion collisions because they can leave the reaction volume essentially undistorted by final-state interactions. Indeed, dileptons from heavy-ion collisions have been measured by the DLS collaboration at the BEVALAC [5, 6, 7] and by the CERES [8], HELIOS [9, 10], NA38 [11] and NA50 collaborations [12] at SPS energies.

The recent data on e^+e^- or $\mu^+\mu^-$ spectra at SPS energies might provide valuable insight; Li et al. [13] have proposed that the enhancement of e^+e^- pairs in S + Au collisions as observed by the CERES collaboration [8] stems from an enhanced ρ-meson production (via $\pi^+\pi^-$ annihilation) due to a dropping ρ-mass in the medium. In fact, their analysis – which is based on an expanding fireball scenario – is supported by the microscopic transport calculations in ref. [14]. Meanwhile various authors have substantiated the observation of refs. [13, 14], *i.e.* that the spectral shape of the dilepton yield is incompatible with 'free' meson form factors [15, 16, 17, 18, 19]. However, a more conventional approach including the change of the ρ-meson spectral function in the medium due to the coupling of ρ, π, Δ and nucleon dynamics along the lines of refs. [20, 21, 22, 23] was found to be (roughly) compatible with the CERES data [14, 23], as well, whereas the dimuon data of the HELIOS-3 collaboration [9] could only be described satisfactorily when including 'dropping' meson masses [24, 25]. Meanwhile, our knowledge on the ρ spectral function has improved since – as first pointed out by Friman and Pirner [26] - resonant ρ-N interactions in p-wave scattering significantly enhance the strength in the vector-isovector channel at low invariant mass. In fact, the CERES data for S + Au at 200 A GeV and Pb + Au at 160 A GeV, using an expanding fireball model, were found to be compatible within such a hadronic scenario [27].

In the present work we report on novel developments in this direction by improving on both the reaction dynamics and the ρ spectral function (*e.g.* by constraints from γp data), which will be discussed in sect. 2. In sect. 3 the resulting dilepton spectra are then compared to the data from both CERES and HELIOS-3 collaborations simultaneously; we also search for observables that might distinguish between the 'hadronic' and 'dropping mass' scenario, in particular dilepton q_T-spectra and inclusive yields *above* the ρ mass. We finish with a summary and concluding remarks in sect. 4.

2 Heavy-Ion Reaction Dynamics and in-Medium Rho Propagator

The dynamical description of proton-nucleus or nucleus-nucleus collisions is performed within the covariant transport approach HSD [28] which has been found to account for hadronic data from SIS to SPS energies reasonably well and has recently been used in the analysis of dilepton data [14, 24, 29]. The dilepton production is calculated perturbatively by including the contributions from the Dalitz-decays $\eta \to \gamma l^+l^-$, $\omega \to \pi^0 l^+l^-$, $\eta' \to \gamma l^+l^-$ and the direct dilepton decays of the vector mesons ρ, ω and ϕ where the ρ and the ϕ meson may as well be produced in $\pi^+\pi^-$ and $K\bar{K}$ or $\pi\rho$ collisions, respectively. For a detailed description of all these processes we refer the reader to ref. [29]. We note that we discard baryon-baryon (BB), meson-baryon (mB) and meson-meson (mm) bremsstrahlung channels as well as the Dalitz decays of the baryon resonances in order to avoid double counting when employing the full ρ spectral function.

The dilepton radiation from ρ mesons is calculated as

$$\frac{dN_{l^+l^-}}{dM} = -\frac{2M}{\pi}\ \mathrm{Im}D_\rho(q_0, q; \rho_B, T) \tag{1}$$

where D_ρ is the ρ-meson propagator in the hadronic medium, depending on the baryon density ρ_B and temperature T as well as on energy q_0 and 3-momentum $q \equiv |\vec{q}|$ in the local rest frame of the baryon current ('comoving' frame). The invariant mass M is related to the ρ-meson 4-momentum in the nuclear medium as

$$M^2 = q_0^2 - q^2\ , \tag{2}$$

while

$$\mathrm{Im}D_\rho = \frac{1}{3}(\mathrm{Im}D_\rho^L + 2\mathrm{Im}D_\rho^T) \tag{3}$$

is spin averaged over the longitudinal and transverse part of the ρ-propagator:

$$\mathrm{Im}D_\rho^{L,T}(q_0, q; \rho_B, T) = \frac{\mathrm{Im}\Sigma_\rho^{L,T}(q_0, q; \rho_B, T)}{|M^2 - (m_\rho^{bare})^2 - \Sigma_\rho^{L,T}(q_0, q; \rho_B, T)|^2}\ . \tag{4}$$

The ρ-meson selfenergy $\Sigma_\rho^{L,T}(q_0, q; \rho_B, T)$ is obtained by combining the effects of the different hadronic interactions as:

$$\Sigma_\rho^L = \Sigma_{\rho\pi\pi} + \Sigma_{\rho\pi a_1}^L + \Sigma_{\rho K K_1}^L + \Sigma_{\rho\bar{K}\bar{K}_1}^L \tag{5}$$

$$\Sigma_\rho^T = \Sigma_{\rho\pi\pi} + \Sigma_{\rho BB^{-1}} + \Sigma_{\rho\pi a_1}^T + \Sigma_{\rho K K_1}^T + \Sigma_{\rho\bar{K}\bar{K}_1}^T\ . \tag{6}$$

The explicit evaluation of the various selfenergy components is discussed in detail in ref. [27]. We here employ an improved version in the following respects:

a) in addition to p-wave $\rho N \to B$ interactions (B=N, Δ, $N(1720)$ and $\Delta(1905)$) we also account for s-wave excitations into $N(1520)$ and $\Delta(1700)$ resonances (as usual, the corresponding coupling constants are estimated from the ρN partial decay width);

b) the coupling of the resonances to virtual photons is calculated within the improved vector dominance model of Kroll, Lee and Zumino [30] to avoid overestimates of the $B \to N\gamma$ branching ratios;

c) the medium modifications of the two-pion selfenergy $\Sigma_{\rho\pi\pi}$ are extended to arbitrary 3-momentum within the recently developed model of Urban *et al.* [31].

The combined ρ-meson selfenergy is then further constrained by experimental information on γp and γA absorption cross sections [32] which correspond to the limit $M^2 \to 0$. The constraints by photo-production data have been stressed by several authors [33, 29, 19, 34, 35, 36] and thus qualify as stringent benchmarks for the ρ spectral function. We note that by resummation of hadronic interactions in the ρ-meson selfenergy Σ_ρ (eqs. (5),(6)) we incorporate dynamical effects which are not only linear in the baryon density ρ_B, but also of higher order. The resummation of interactions at fixed baryon density and temperature involves the assumption that all interaction terms add coherently – an assumption that might become questionable due to the short time scales of a few fm/c in heavy-ion collisions at SPS energies [28]. Our approach thus differs conceptually from the analysis performed in Refs. [35, 36] where only dilepton rates linear in ρ_B have been considered and higher order coherent effects have been discarded.

As an example – relevant for the heavy-ion reactions at SPS energies – we show in Fig. 1 the spin averaged $-\mathrm{Im}D_\rho(q_0, q; \rho_B, T)$ as a function of the invariant mass M and the 3-momentum q for a temperature of 150 MeV at $\rho_B = 0, \rho_0, 2\rho_0$ and $3\rho_0$, respectively. With increasing baryon density we find the ρ spectral function to increase substantially in width showing only minor structures at high density. Thus the lifetime of the ρ-meson in the nuclear medium becomes very short due to well established hadronic interactions. As a consequence, its average propagation in space is limited to distances less than 0.5 fm already at normal nuclear matter density (even for high momenta).

The cross section for the pion annihilation channel $\pi^+\pi^- \to \rho^0 \to e^+e^-$ is taken in line with ref. [37] as

$$\sigma_{\pi^+\pi^-\to e^+e^-}(M) = -\frac{16\pi^2\alpha^2}{g^2_{\rho\pi\pi}} \frac{1}{k^2M^2} (m_\rho^{bare})^4 \mathrm{Im}D_\rho(q_0, q; \rho_B, T) , \tag{7}$$

where $k = (M^2 - 4m_\pi^2)^{1/2}/2$ is the pion 3-momentum in the center-of-mass frame and α is the fine structure constant. The $\rho\pi\pi$ coupling constant and bare ρ mass are fixed to reproduce the pion electromagnetic form factor in free space [27].

In this way we ensure that the Fourier transformation of the isovector current-current correlation function in vacuum is consistent with the experimental information in terms of the vacuum ρ spectral function [35]. We note that constraints from chiral symmetry are not fully accounted for in our model for the spectral function since the $a_1(1260)$ meson is not treated as the chiral partner of the ρ meson [19]. However, the dominant effects arise from p-wave πN- and resonant ρN scattering, where chiral symmetry does not play a dominant role.

Our dynamical calculations are carried out as follows: the time-evolution of the proton-nucleus or nucleus-nucleus collision is described within the covariant transport

approach HSD [28, 29] without dropping vector meson masses. Whenever a ρ-meson is produced in the course of the hadronic cascade (by baryon-baryon, meson-baryon or pion-pion collisions), its 4-momentum in the local rest frame of the baryon current is recorded together with the information on the local baryon density, the local 'transverse' temperature and its production source. We note that the definition of a local temperature is model dependent; here we have used a logarithmic fit to the transverse p_t spectra of mesons at midrapidity. Without going into a detailed discussion of this issue we note that our results for dilepton spectra do not change within the numerical accuracy when using a constant temperature $T = 150$ MeV at SPS energies since $\mathrm{Im}D_\rho$ depends rather weakly on T (at a given nucleon density).

3 Comparison to HELIOS-3 and CERES Data

We begin our discussion of the dilepton spectra at SPS energies with the p + W system at 200 GeV incident energy. Fig. 2 shows the spectral channel decomposition as a function of the $\mu^+\mu^-$ invariant mass M in comparison to the data of the HELIOS-3 collaboration [9] including the experimental cuts in transverse mass and rapidity as well as the experimental mass resolution as in ref. [24]. The spectrum is normalized to the charged particle multiplicity N_c in the pseudorapidity bin $3.7 \leq \eta \leq 5.2$. The upper part of Fig. 2 shows the dimuon spectra when employing the 'free' ρ spectral function whereas the lower part displays our results when accounting for the full medium modifications of the ρ-meson propagator. As is apparent from Fig. 2, the spectrum for p + W can be fully accounted for by the electromagnetic decays of the η, η' and vector mesons ρ^0, ω and ϕ; contributions from meson-meson channels ($\pi^+\pi^-, K\bar{K}, \pi\rho$) are of minor importance here. Furthermore, since the ρ-meson essentially hadronizes in the vacuum, there is no noticeable difference between the summed spectra in the upper and lower part of Fig. 2.

The situation changes appreciably when turning to nucleus-nucleus collisions. In Fig. 3 we compare the results of our calculation for the differential dilepton spectra for S + W at 200 A·GeV with the experimental data [9] employing the same cuts and mass resolution as before. Again, the upper part shows our results for the 'free' ρ spectral function whereas the lower part represents our results including the full medium modifications of the ρ propagator. Even at forward rapidities as measured in central S + W (200 A·GeV) a sizable contribution for invariant masses 0.3 GeV $\leq M \leq$ 0.7 GeV stems from the $\pi^+\pi^- \to \rho \to \mu^+\mu^-$ channel. Also in the ϕ mass regime around 1 GeV there is a significant contribution from $K\bar{K}$ and $\pi\rho$ annihilation to dimuons which explains the enhanced $\phi/(\rho+\omega)$ ratio in S + W relative to p + W. As has been found earlier [24, 25] the experimental spectrum cannot be properly described in terms of a 'free' ρ spectral function: there is an excess for invariant masses $M \approx 0.8$ GeV and insufficient yield around $M \approx 0.5$ GeV. The description of the data is significantly improved when including the hadronic medium modifications of the ρ propagator (lower part of Fig. 3) – quite analogous to the 'dropping mass' scenario [24] when employing a ρ-mass shift according to Hatsuda and Lee [38]. However, there persists a significant difference: whereas in the 'dropping mass' scenario (cf. Fig. 4

of ref. [24]) the dimuon yield is underestimated for $M \geq 1.2$ GeV the in-medium ρ spectral function seems to give sufficient pairs in this region due to its substantial broadening in dense matter (cf. Fig. 1).

In Fig. 4 we also compare the results of our calculation for the differential dilepton spectra in Pb + Au at 160 A·GeV and $b = 5$ fm with preliminary experimental data [39, 40]. The e^+e^- acceptance cuts in pseudorapidity ($2.1 \leq \eta \leq 2.65$), transverse momentum ($p_T \geq 0.175$ GeV/c) as well as in the opening angle of the e^+e^- pair ($\Theta \geq 35$ mrad) are taken into account. Furthermore, the experimental mass resolution has been included in evaluating the final mass spectrum, which is normalized to the number of charged particles $dn_{ch}/d\eta$ in the pseudorapidity bin $2.1 \leq \eta \leq 3.1$. Again, the upper part shows our results for the 'free' ρ spectral function whereas the lower part represents our results including the full medium modifications. For Pb + Au at 160 A·GeV (and semi central collisions) the dominant yield for invariant masses $0.3 \leq M \leq 0.7$ GeV stems from $\pi^+\pi^-$ annihilation. In the ϕ mass regime around 1 GeV there is again a large contribution from $K\bar{K}$ and $\pi\rho$ annihilation to dileptons. Within the present statistics, however, there is no unique signal for in-medium effects since the calculation with the 'free' spectral function (upper part) also describes the data except for one point at 0.7 GeV (cf. also ref. [17]). The calculation with the full spectral function describes the data somewhat better to the same accuracy as within the 'dropping mass' scenario [29]. We note that the comparison with the data in Fig. 4 has been performed for impact parameter $b = 5$ fm, for which our transport model gives a charged particle multiplicity $dn_{ch}/d\eta \approx 260$ in accordance with the experimental normalization.

Since the present dilepton invariant mass spectra do not discriminate the different models we also explore if the momentum distributions of the lepton pairs give some further insight (as suggested by Friman and Pirner [26] and in ref. [29]). Our calculated transverse momentum spectra – integrated over rapidity and the invariant mass range $0.3 \leq M \leq 0.7$ GeV – are shown in Fig. 5 for Pb + Au at 160 A·GeV and $b = 2$ fm using q_T-bins of 50 MeV/c. The dashed line in Fig. 5 displays the result with the 'free' spectral function while the solid line shows the result for the in-medium spectral function. Apart from an overall increase of the spectrum we do *not* observe significant changes of the slope in q_T – as was the case for the 'dropping mass' scenario (cf. Fig. 13 of ref. [29]). Thus, the q_T spectra do not qualify in disentangling the different schemes either.

Another signature studied in ref. [29] and also suggested in [36] is related to the total dilepton yield between the free ω and ϕ peaks where the dominant contribution stems from ρ decays. In this regime the 'dropping mass' scenario leads to a *reduction* by about a factor 2-3 as compared to a 'free' ρ spectral function for Pb + Pb at 160 A·GeV [29], while a broadening of the ρ spectral function due to hadronic interactions shows an *enhancement*. This feature is demonstrated quantitatively in Fig. 6 for Pb + Au at b=5 fm for the different scenarios employing an experimental mass resolution of ΔM=10 MeV. We find a difference by about a factor of 5 between the 'dropping mass' scenario (dashed line) and the hadronic spectral function approach (solid line) which might be accessible experimentally with the CERES detector at improved mass resolution. We note, furthermore, that in the spectral function approach

the relative enhancement is most pronounced at $M \simeq 0.3$ GeV while in the dropping mass scheme we find a maximum enhancement at $M \simeq 0.5$ GeV for this system.

4 Summary

On the basis of the covariant transport approach HSD [28, 29] we have studied dilepton production in proton and heavy-ion induced reactions at SPS energies. Various contributions are accounted for: the Dalitz-decays of η, ω, η' mesons, the direct dilepton decays of the vector mesons ρ, ω and ϕ as well as $K\bar{K}$ and $\pi\rho$ channels. It is found that for p + W collisions at 200 GeV the mesonic decays almost completely determine the dilepton yield, whereas in S + W and Pb + Au reactions the $\pi^+\pi^- \to \rho \to l^+l^-$, $K\bar{K} \to \phi \to l^+l^-$ annihilation channels and $\pi\rho$ collisions contribute substantially. The experimental data taken by the HELIOS-3 [9] and CERES collaborations [8, 39, 40] are in general underestimated by the calculations for invariant masses 0.35 GeV $\leq M \leq$ 0.65 GeV when using a 'free' ρ spectral function (in accordance with refs. [13, 15, 25]).

It turns out that both the 'dropping mass' scenario – using either Brown/Rho scaling [13, 25] or dropping vector meson masses according to QCD sum rule studies [14, 24, 29] – as well as the hadronic spectral function approach [27] lead to dilepton spectra that are in good agreement with the experimental data for all systems at SPS energies (cf. also ref. [40]). In order to discriminate between the different models we have investigated dilepton transverse momentum distributions for invariant masses $0.3 \leq M \leq 0.7$ GeV in Pb + Au collisions; unfortunately, only little differences have been found as compared to the dropping mass scenario [29]. However, the in-medium broadening of the ρ spectral function results in a much higher dilepton rate than the dropping mass scenario *above* the ω-mass. Therefore one might experimentally distinguish the two different scenarios by the total dilepton yield in the invariant mass range $0.8 \leq M \leq 1$ GeV in Pb + Au collisions (cf. Fig. 6), provided that the experimental mass resolution is on the order of about 10 MeV.

Acknowledgement

The authors are grateful for many helpful discussions with G.E. Brown, A. Drees, C. M. Ko and U. Mosel. We are indebted to M. Urban for providing us with results on the finite 3-momentum dependence in the two-pion selfenergy. One of us (RR) acknowledges support from the Alexander-von-Humboldt foundation as a Feodor-Lynen fellow. This work was supported in part by the U.S. department of energy under contract No. DE-FG02-88ER40388 and by the National Science Foundation, NSF PHY 94-21309 .

References

[1] G. Brown and M. Rho, Phys. Rev. Lett. 66 (1991) 2720.

[2] M. C. Birse, J. Phys. G20 (1994) 1537.

[3] G. Q. Li, C. M. Ko, and X. S. Fang, Phys. Lett. B329 (1994) 149.

[4] W. Cassing, E. L. Bratkovskaya, U. Mosel, S. Teis, and A. Sibirtsev, Nucl. Phys. A614 (1997) 415.

[5] G. Roche et al., Phys. Rev. Lett. 61 (1988) 1069.

[6] C. Naudet et al., Phys. Rev. Lett. 62 (1989) 2652.

[7] G. Roche et al., Phys. Lett. B226 (1989) 228.

[8] G. Agakichiev et al., Phys. Rev. Lett. 75 (1995) 1272.

[9] M. A. Mazzoni, Nucl. Phys. A566 (1994) 95c; M. Masera, Nucl. Phys. A590 (1995) 93c.

[10] T. Åkesson et al., Z. Phys. C68 (1995) 47.

[11] C. Baglin et al., NA38, Phys. Lett. B220 (1989) 471; B251 (1990) 465.

[12] M. Gonin et al., Nucl. Phys. A610 (1996) 404c.

[13] G. Q. Li, C. M. Ko, and G. E. Brown, Phys. Rev. Lett. 75 (1995) 4007.

[14] W. Cassing, W. Ehehalt, and C. M. Ko, Phys. Lett. B363 (1995) 35.

[15] V. Koch and C. Song, Phys. Rev. C54 (1996) 1903.

[16] D. K. Srivastava, B. Sinha, and C. Gale, Phys. Rev. C53 (1996) R567.

[17] L. A. Winckelmann, C. Ernst, L. Gerland, J. Konopka, S. Soff et al., nucl-th/9610042.

[18] J. Sollfrank, P. Huovinen, M. Kataja, P.V. Ruuskanen, M. Prakash, and R. Venugopalan, Phys. Rev. C55 (1997) 392.

[19] C.M. Hung and E.V. Shuryak, Phys. Rev. C 56 (1997) 453.

[20] M. Herrmann, B. Friman, and W. Nörenberg, Nucl. Phys. A560 (1993) 411.

[21] M. Asakawa, C. M. Ko, P. Lévai, and X. J. Qiu, Phys. Rev. C46 (1992) R1159.

[22] G. Chanfray and P. Schuck, Nucl. Phys. A545 (1992) 271c.

[23] R. Rapp, G. Chanfray, and J. Wambach, Phys. Rev. Lett. 76 (1996) 368.

[24] W. Cassing, W. Ehehalt, and I. Kralik, Phys. Lett. B377 (1996) 5.

[25] C. M. Ko, G. Q. Li, G. E. Brown, and H. Sorge, Nucl. Phys. A610 (1996) 342c.

[26] B. Friman and H. J. Pirner, Nucl. Phys. A617 (1997) 496.

[27] R. Rapp, G. Chanfray and J. Wambach, Nucl. Phys. A617 (1997) 472.

[28] W. Ehehalt and W. Cassing, Nucl. Phys. A602 (1996) 449.

[29] E. L. Bratkovskaya and W. Cassing, Nucl. Phys. A619 (1997) 413.

[30] N.M. Kroll, T.D. Lee and B. Zumino, Phys. Rev. 157 (1967) 1376.

[31] M. Urban *et al.*, private communication and to be published.

[32] R. Rapp, M. Urban, M. Buballa and J. Wambach, nucl-th/9709008.

[33] A. Drees, Phys. Lett. B388 (1997) 380.

[34] G.Q. Li and G.E. Brown, nucl-th/9706076.

[35] J.V. Steele, H. Yamagishi, and I. Zahed, Phys. Lett. B384 (1996) 255.

[36] J.V. Steele, H. Yamagishi, and I. Zahed, hep-ph/9704414v2.

[37] P. Koch, Z. Phys. C57 (1993) 283.

[38] T. Hatsuda and S. Lee, Phys. Rev. C46 (1992) R34.

[39] Th. Ullrich et al., Nucl. Phys. A610 (1996) 317c;

[40] A. Drees, Nucl. Phys. A610 (1996) 536c.

Figure Captions

Fig. 1: The (negative) imaginary part of the ρ propagator averaged over the longitudinal and transverse components as a function of the invariant mass M and the momentum q for baryon densities of 0, 1 ρ_0, 2 ρ_0, and 3 ρ_0 and temperature $T = 150$ MeV. Note the different absolute scales in the individual figures.

Fig. 2: The calculated dimuon spectra (full solid line) for p + W at 200 A·GeV in comparison with the data from ref. [9]. The thin lines indicate the individual contributions from the different production channels including the HELIOS-3 acceptance and mass resolution; *i.e.* starting from low M: $\eta \to \gamma e^+e^-$ (dashed line), $\omega \to \pi^0 e^+e^-$ (dot-dashed line), $\eta' \to \gamma e^+e^-$ (long dashed line); for $M \approx 0.8$ GeV: $\omega \to e^+e^-$ (dot-dot-dashed line), $\rho^0 \to e^+e^-$ (dashed line), $\pi^+\pi^- \to \rho \to e^+e^-$ (dot-dashed line); for $M \approx 1$ GeV: $\phi \to e^+e^-$ (dot-dashed line), $\pi\rho \to e^+e^-$ (dot-long dashed line), $K\bar{K} \to e^+e^-$ (dashed line). The upper part shows the result for a 'free' ρ spectral function whereas the lower part is obtained for the full ρ spectral function.

Fig. 3: Dimuon invariant mass spectra for central collisions of S + W at 200 A·GeV (full solid lines) in comparison to the data of the HELIOS-3 collaboration [9]. The upper part shows the results of a calculation with a 'free' ρ spectral function whereas the lower part includes the full ρ spectral function as described in the text. The assignment of the individual contributions is the same as in Fig. 2.

Fig. 4: Dielectron invariant mass spectra for semi central collisions of Pb + Au at 160 A·GeV (full solid lines) in comparison to the preliminary data of the CERES collaboration [39]. The upper part shows the results of a calculation with a 'free' ρ spectral function whereas the lower part includes the full ρ spectral function as described in the text. The assignment of the individual contributions is the same as in Fig. 2.

Fig. 5: The dielectron transverse momentum distribution for the invariant mass range $0.3 \leq M \leq 0.7$ GeV for Pb + Au at 160 A·GeV at $b = 5$ fm for the 'free' ρ spectral function (dotted line) and with our in-medium spectral function (solid line).

Fig. 6: The dielectron invariant mass spectra for Pb + Au at 160 A·GeV at $b = 5$ fm for the 'free' ρ spectral function (dotted line) and with our in-medium spectral function (solid line). The dashed line corresponds to the 'dropping mass' scenario investigated in ref. [29].

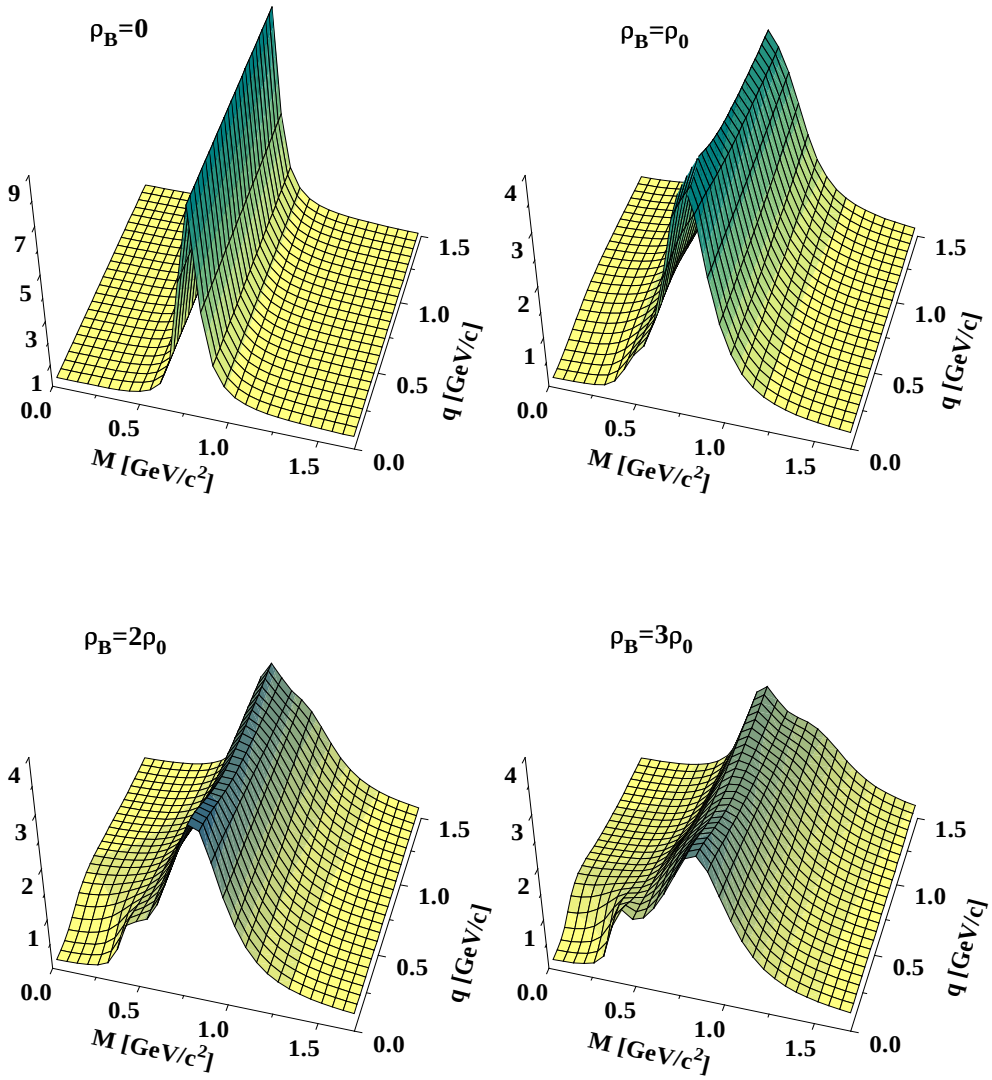
-Im D$_\rho$ (M,q,ρ_B,T) [GeV^{-2}]
T=150 MeV
ρ_B=0
ρ_B=ρ_0
ρ_B=2ρ_0
ρ_B=3ρ_0
M [GeV/c^2]
q [GeV/c]

Fig. 1

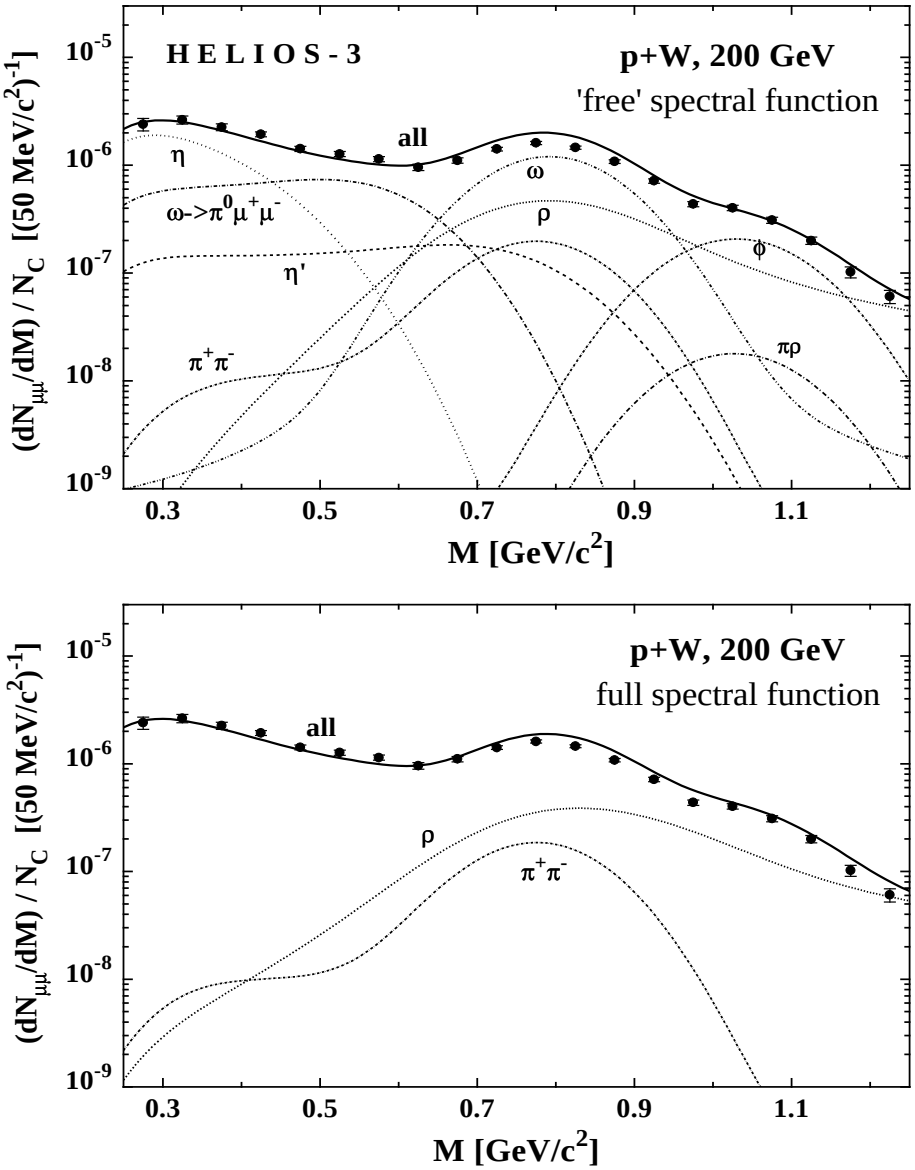
H E L I O S - 3
p+W, 200 GeV
'free' spectral function
all
η
ω
ρ
ω->π0μ+μ-
η'
ϕ
π+π-
πρ
(dNμμ/dM) / NC [(50 MeV/c2)-1]
M [GeV/c2]
p+W, 200 GeV
full spectral function
all
ρ
π+π-
(dNμμ/dM) / NC [(50 MeV/c2)-1]
M [GeV/c2]

Fig. 2

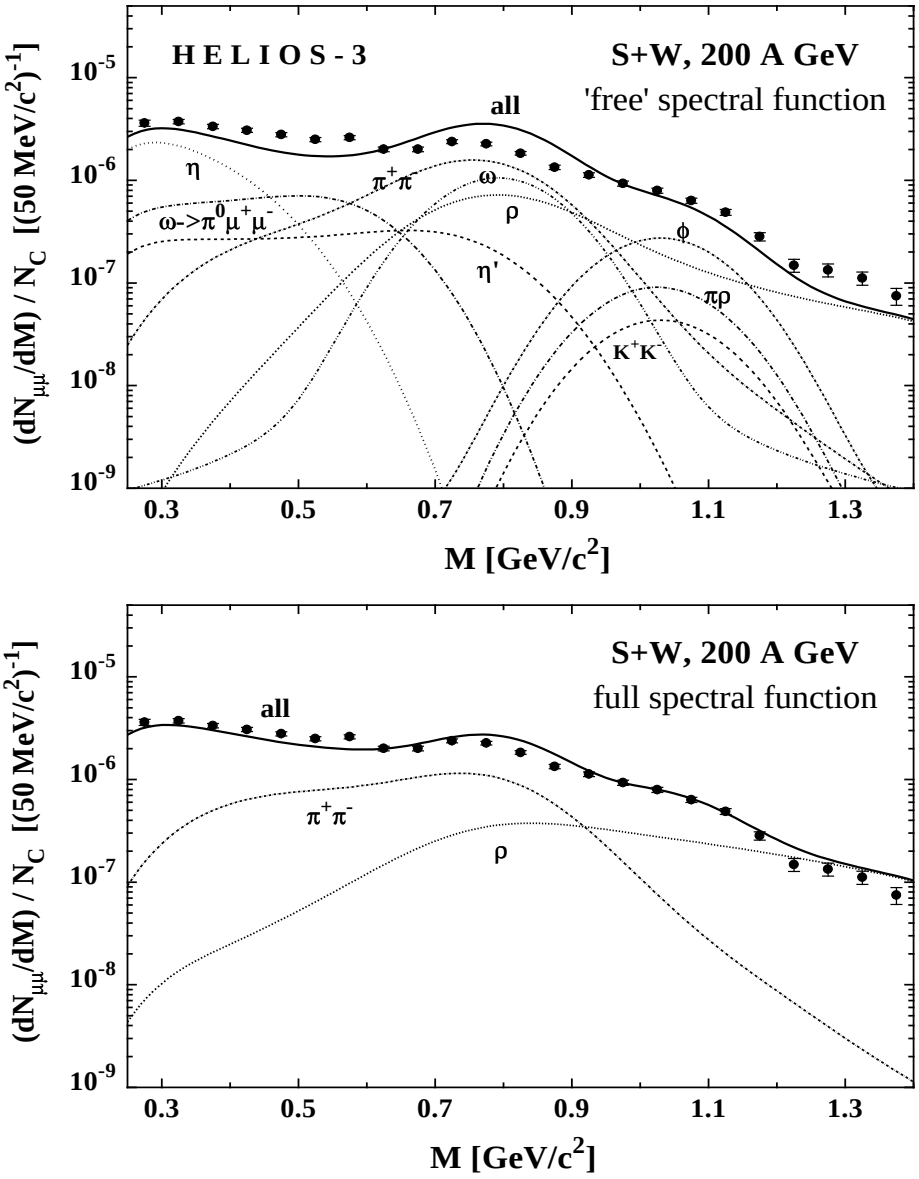
H E L I O S - 3
S+W, 200 A GeV
'free' spectral function
all
η
π+π-
ω
ρ
ω->π0μ+μ-
η'
ϕ
πρ
K+K-
(dNμμ/dM) / NC [(50 MeV/c2)-1]
M [GeV/c2]
S+W, 200 A GeV
full spectral function
all
π+π-
ρ
(dNμμ/dM) / NC [(50 MeV/c2)-1]
M [GeV/c2]

Fig. 3

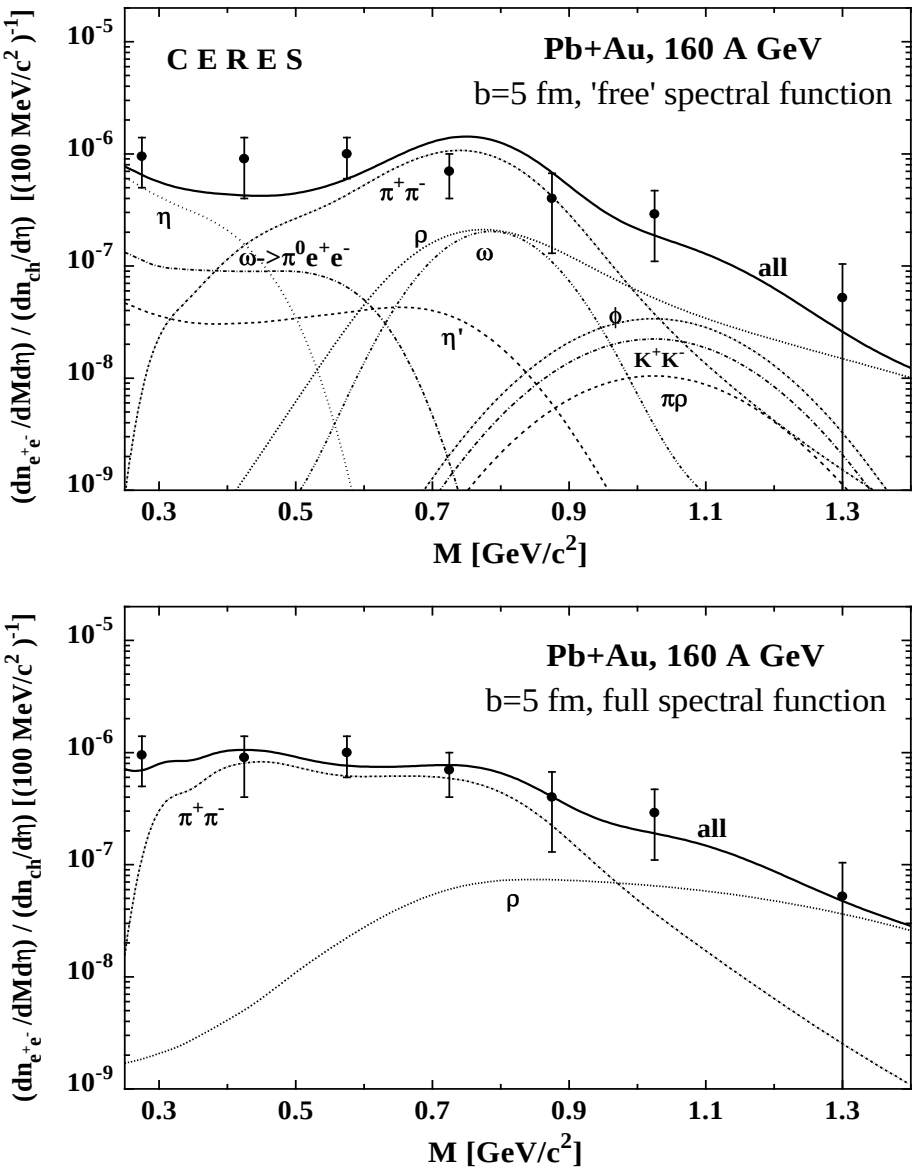
CERES
Pb+Au, 160 A GeV
b=5 fm, 'free' spectral function
η
π+π-
ρ
ω
ω->π0e+e-
η'
φ
K+K-
πρ
all
(dne+e-/dMdη) / (dnch/dη) [(100 MeV/c2)-1]
M [GeV/c2]
Pb+Au, 160 A GeV
b=5 fm, full spectral function
π+π-
ρ
all
(dne+e-/dMdη) / (dnch/dη) [(100 MeV/c2)-1]
M [GeV/c2]

Fig. 4

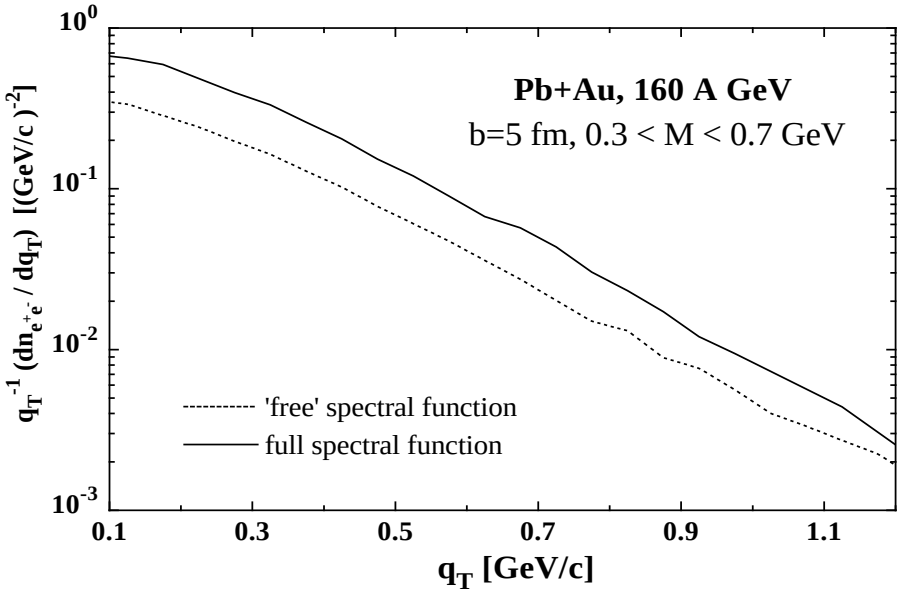
Pb+Au, 160 A GeV
b=5 fm, 0.3 < M < 0.7 GeV
'free' spectral function
full spectral function
q_T^{-1} ($dn_{e^+e^-}$ / dq_T) [(GeV/c)$^{-2}$]
q_T [GeV/c]
10^0
10^{-1}
10^{-2}
10^{-3}
0.1
0.3
0.5
0.7
0.9
1.1

Fig. 5

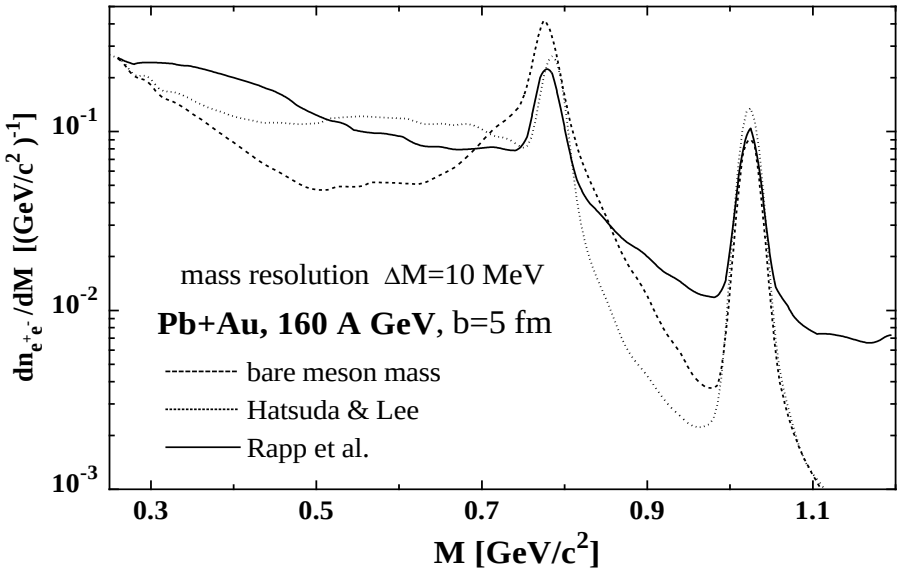
mass resolution ΔM=10 MeV
Pb+Au, 160 A GeV, b=5 fm
bare meson mass
Hatsuda & Lee
Rapp et al.
dn_e+e-/dM [(GeV/c^2)^-1]
M [GeV/c^2]
10^-1
10^-2
10^-3
0.3
0.5
0.7
0.9
1.1

Fig. 6